Lecture

Leber Congenital Amaurosis (LCA): Potential for Improvement of Vision

Artur V. Cideciyan and Samuel G. Jacobson

Scheie Eye Institute, Department of Ophthalmology, Perelman School of Medicine, University of Pennsylvania, Philadelphia, Pennsylvania, United States

Correspondence: Artur V. Cideciyan, Scheie Eye Institute, 51 North 39th Street, Philadelphia, PA 19104, USA; cideciya@pennmedicine.upenn.edu.
Samuel G. Jacobson, Scheie Eye Institute, 51 North 39th Street, Philadelphia, PA 19104, USA; jacobsos@pennmedicine.upenn.edu.

Citation: Cideciyan AV, Jacobson SG. Leber congenital amaurosis (LCA): potential for improvement of vision. *Invest Ophthalmol Vis Sci*. 2019;60:1680–1695. https://doi.org/10.1167/iovs.19-26672

Leber congenital amaurosis (LCA) is a group of monogenic inherited retinal degenerations that typically show early onset and severe visual dysfunction. In addition, there is a natural history of progressive loss of photoreceptors and associated further loss of vision. The therapeutic goal of slowing the natural history of degenerative disease has a long history of effort and deserves our attention, but it is imperative to have realistic timelines and careful protocols that define how efficacy will be measured over many years. The therapeutic goal of improving vision is easier to detect over a shorter period of observation. However, modern techniques of noninvasive examination in LCA have demonstrated that only a subset of patients can be predicted to have potential for improvement of vision, given safe and effective therapies. Discussed herein are two LCA subtypes, the ciliopathy of *CEP290*-LCA and the phototransduction defect of *GUCY2D*-LCA, that show a common potential for improvement of vision despite differences in molecular mechanism.

Mutations in several hundred genes are now known to cause inherited retinal diseases (IRDs).[1–4] IRDs represent a highly heterogeneous group of disorders that have one common element: abnormal visual function originating at the level of retinal photoreceptors. A subset of IRDs comprises syndromic diseases, whereas the majority are nonsyndromic and affect only the retina even when the gene is expressed ubiquitously. The source of photoreceptor dysfunction can be due to maldevelopment of cells,[5,6] a defect in the neighboring retinal pigment epithelium (RPE) cells,[7,8] progressive loss of cells to neurodegeneration,[9] a variety of other pathophysiological mechanisms,[10] or a combination thereof. Until a decade ago, IRDs were treated mainly with nutrient supplements aimed to slow the disease.[11] Then, converging information from molecular and retinal biology, animal models, human phenotyping, and therapeutic tools reached a critical mass,[12–19] and led to the first successful proof of concept of a gene-based treatment of an IRD caused by *RPE65* mutations.[20–23] Extensive research followed to describe the extent and the source of improvement of visual function, durability of the treatment, and the effects on the rate of photoreceptor degeneration.[24–30] Recent approval of this gene therapy approach for marketing in the United States and Europe[31] has generated greater interest in the development of treatments for other IRDs.

There is no one-size-fits-all approach to gene-based treatments for IRDs. Therapeutic directions for different IRDs need to be aligned with the underlying molecular pathophysiology, with the tools available for their delivery, and with consideration of the recipient retinal cells expected to be retained at the time of the intervention. For example, larger genes cannot be packaged into some viral vectors,[32] or rod photoreceptor-based treatments would not be appropriate for adult patients with Class A rhodopsin mutations who have only cones remaining.[33] Outcome measures also need to be optimized to the expected magnitude and timing of the efficacy signal. For example, evidence for successful slowing of disease progression may take years to detect[34,35] but improvements in vision may occur in days to weeks.[22,36]

Among the more severe IRDs are those clinically classified as LCA. LCA manifests vision loss that usually occurs congenitally or in early infancy. There is nystagmus (involuntary eye movements), and a deceptively benign fundus appearance at early stages, but the disease expression tends to be indistinguishable from that of other IRDs at later stages. Abnormal electroretinograms localize the vision defect to the outer retina, at the photoreceptors. The attraction of some forms of LCA as a target for therapy rests not only in the severity of the vision loss but also in the key fact that improvement of visual function is potentially achievable because there is evidence of dissociation of function and structure.[16] The first form of LCA with sufficient proof of concept research, understanding of molecular mechanism, and detailed pretreatment human disease characterization indicating structural preservation but severe functional losses was the RPE disease with a defective retinoid cycle: *RPE65*-LCA.[25] The improved vision in *RPE65*-LCA patients post therapy in three clinical trials conducted independently but almost simultaneously, is in contrast to the results in another RPE-based severe and early-onset IRD caused by mutations in *MERTK*. Despite longstanding rodent proof of concept research and understanding of mechanism, there was limited characterization of the human disease and no published demonstration of structure–function dissociation. A clinical trial protocol mimicking that of the *RPE65*-LCA trials in *MERTK* patients failed to achieve the efficacy results of *RPE65*-LCA.[37]

Two photoreceptor diseases within the clinical category of LCA, *CEP290*-LCA and *GUCY2D*-LCA, have been shown to have a dissociation of structure and function in affected humans and thus are good candidates for appropriate vision improving therapies.[38–45]

CEP290-LCA

Photoreceptor Cilium and LCA-Ciliopathies

Rod and cone photoreceptors are specialized cells for phototransduction, and this process converts light into neural signals and vision. Photoreceptors have four major compartments: the outer and inner segments, the cell body, and the synaptic terminal (Fig. 1A). As part of their specialization, the photoreceptors contain one of the longest sensory cilia known in mammalian cells, extending across the inner and outer segments. Between the inner and outer segments of photoreceptors is the ciliary transition zone, also called the connecting cilium, which can be thought of as a two-way highway for the trafficking of all the proteins to and from the outer segment, where phototransduction takes place, and a gate that allows appropriate compartmentalization of proteins (Figs. 1B, 1C).

It has been long hypothesized that the connecting cilium may be a primary site of disease in some inherited retinopathies,[46] and now it is known that large numbers of IRD genes are expressed at the connecting cilium.[47,48] Indeed, at least one-third of the molecular pathways known to be associated with syndromic or nonsyndromic forms of LCA are thought to be ciliopathies.[49–51] *CEP290* (centrosomal protein, 290 kD) gene encodes a large protein that is located at the transition zone of the rod photoreceptors[52,53] (Fig. 1D), and mutations in *CEP290* are among the most common genetic causes of LCA.[54–56] CEP290 is also expressed in primate cone photoreceptors (Fig. 1E).

Visual Consequences

LCA is generally considered more severe than other IRDs such as retinitis pigmentosa (RP). However, even within LCA, different molecular subtypes can show substantial differences in severity. Defining severe vision loss as a visual acuity of counting fingers (CF) or worse in the best-seeing eye, 62% to 89% of patients with *CEP290*-LCA have severe vision loss,[38,39,57–61] whereas this proportion is closer to 10% in *RPE65*-LCA.[57,62,63] Importantly, many *CEP290*-LCA patients report very low level of vision from as early as they can remember, implying a congenital lack of visual functioning. Consistent with congenital or very early-onset vision loss are the large hyperopic refractive errors in *CEP290*-LCA[38,39,58,60] suggesting problems with emmetropization during development.

Although visual acuity is useful and understandable to differentiate among the visual abilities of patients, it does not provide a direct measure of the primary function of photoreceptors—to signal light levels. Sensitivity to light can be quantified for rods and cones by determining the dimmest lights a subject can detect. Standard perimeters use this approach to understand the retinotopic distribution of light sensitivity in eyes fixating to a steady reference. However, oculomotor instability of LCA subjects requires a fixation-independent approach to evaluating light sensitivity, which is achieved with full-field stimulus testing (FST).[64,65] In FST each stimulus is presented across the full visual field and thus it does not require a stable gaze. Use of two colors and dark-adapted eyes takes advantage of the spectral separation between rods and cones to understand photoreceptor mediation driving the light sensitivity measured. *CEP290*-LCA patients tend to show more than 4 log units of sensitivity loss.[35,39,66] Chromatic sensitivity differences support mediation by long-/middle-wavelength (L/M) sensitive cones in the great majority of the patients, but there can be exceptions.

Oculomotor Control and Fixation

CEP290-LCA patients demonstrate a wide spectrum of oculomotor abnormalities. On the mild end of this spectrum are eyes with retained visual acuity, fixation, and small-amplitude (fine) nystagmus. The severe end of the spectrum includes eyes with congenital lack of light perception, demonstrating wandering eye movements, no ability to hold the eye in primary gaze, and no fixation.[35] We recently developed a video recording protocol using a confocal scanning laser ophthalmoscope (Spectralis HRA; Heidelberg Engineering, Heidelberg, Germany) commonly used for retinal imaging.[35] The oculomotor control and instability (OCI) protocol uses instantaneous distance between the center of the pupil and a stationary reference such as the medial canthus to quantify two parameters over recording epochs of 30 seconds: the offset from primary gaze, and the extent of oculomotor instability (Figs. 2A, 2B). When performed in a dark room with and without a fixation light, OCI results allow distinguishing between open-loop and close-loop conditions, and thus determine any changes to the oculomotor system that may be driven by visual input.

A normal eye in primary (straight-ahead) gaze corresponds to a pupil center position that is on average 13.7 mm temporal and 3.3 mm superior with respect to the medial canthus (Fig. 2A). Excursions of 30° visual angle from primary gaze along the four cardinal meridians result in approximately 4-mm movements of the center of the pupil away from the center (Fig. 2B). To a first approximation, the location of the center of the pupil can thus be used to quantify the gaze position and its stability over time. As demonstrated in a representative subject, normal eyes tend to be very stable with or without fixation (Fig. 2C, upper traces). Individual *CEP290*-LCA patients can have reliable control of gaze position with small-amplitude nystagmus (Fig. 2C, middle traces), or others may have complete lack of oculomotor control with wandering eyes (Fig. 2C, lower traces). Summary of a cohort of *CEP290*-LCA eyes shows a range of oculomotor instability from 0.3 to 3.5 mm without fixation and 0.2 to 3.6 mm with fixation; similarly, mean gaze offset ranged from 0.6 to 5.5 mm without fixation and 0.2 to 6.2 mm with fixation (Fig. 2D).

Photoreceptor Structure

Retinal neurons and glia are laminated into three nuclear layers and two intervening synaptic layers; distal retina contains carefully aligned photoreceptor outer segments interdigitating with RPE apical processes. Many of the cellular and subcellular retinal features demonstrate natural differences in how much they reflect infrared light, and these differences are imaged by optical coherence tomography (OCT).[67,68] More than a decade ago using lower resolution and slower time-domain OCT systems, we showed that *CEP290*-LCA patients with severe vision loss tend to retain macular photoreceptors.[38] Further studies using higher resolution and faster spectral-domain (SD) OCT systems provided greater information and hypotheses on retinal structure that were tested in relevant animal models.[39–43] More recently we have used a clinical ultrahigh resolution (UHR) SDOCT system (Bi-μ; Kowa Company, Ltd., Tokyo, Japan) to better understand microscopic features in *CEP290*-LCA retinas (Fig. 3).

UHR SDOCT of the normal human retina along the horizontal meridian crossing the fovea shows exquisite micron-scale detail of cellular and subcellular structures. Most prominent across the center of the scan is a hyposcattering (dark) band that corresponds to the outer nuclear layer (ONL) containing the nuclei of rod and cone photoreceptors and the Henle fiber layer (Fig. 3A, upper). However, it is important to

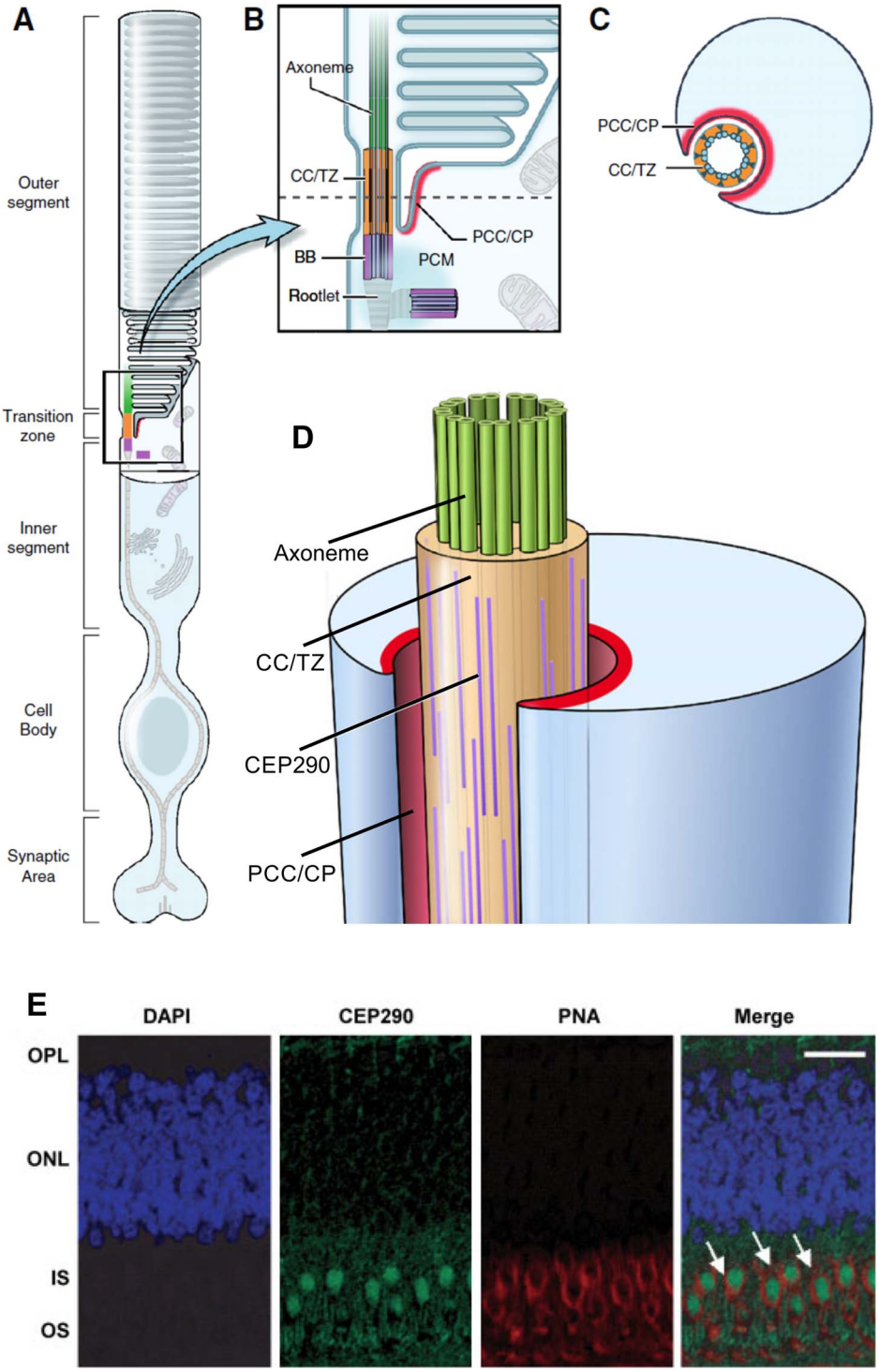

Figure 1. CEP290 expression in rod and cone photoreceptors. (**A**) Schematic of a rod photoreceptor, showing specialized domains of the cell. (**B**) Enlargement of the rod photoreceptor transition zone showing the structural and functional domains in which most ciliary proteins are expressed: axoneme (*green*), connecting cilium/transition zone (CC/TZ; *orange*), basal body (BB; *purple*), periciliary complex or ciliary pocket (PCC/CP; *red*). (**C**) Cross section through the CC/TZ showing the relationship between the microtubules of the cilium and the inner segment, via the PCC/CP. (**A**–**C**) Reprinted and modified with permission from Rachel RA, Li T, Swaroop A. Photoreceptor sensory cilia and ciliopathies: focus on CEP290, RPGR and their interacting proteins. *Cilia*. 2012;1:22. © 2012 The Authors. Published by BioMed Central, Ltd. (**D**) Three-dimensional representation of the transition zone and adjacent domains. Possible positions of rod-like coiled-coil domain proteins such as CEP290, which localize to the region of the Y-linkers between the plasma membrane and the microtubule ring. Reprinted and modified with permission of Rachel RA, Yamamoto EA, Dewanjee MK, et al. *CEP290* alleles in mice disrupt tissue-specific cilia biogenesis and recapitulate features of syndromic ciliopathies. *Hum Mol Genet*. 2015;24:3775–3791. © 2015 The Authors. Published by Oxford University Press. (**E**) Immunofluorescence staining of CEP290 in macular cones of monkey retina. Sections stained with CEP290 (*green*) and cone-specific marker PNA (*red*) indicate colocalization (Merge; *arrows*). DAPI (*blue*) used to stain the nuclei. *Scale bar*: 10 µm. Reprinted with permission from Cideciyan AV, Aleman TS, Jacobson SG, et al. Centrosomal-ciliary gene *CEP290/NPHP6* mutations result in blindness with unexpected sparing of photoreceptors and visual brain: implications for therapy of Leber congenital amaurosis. *Hum Mutat*. 2007;28:1074–1083. © 2007 John Wiley & Sons, Inc. Published by Wiley-Liss, Inc.

Investigative Ophthalmology & Visual Science

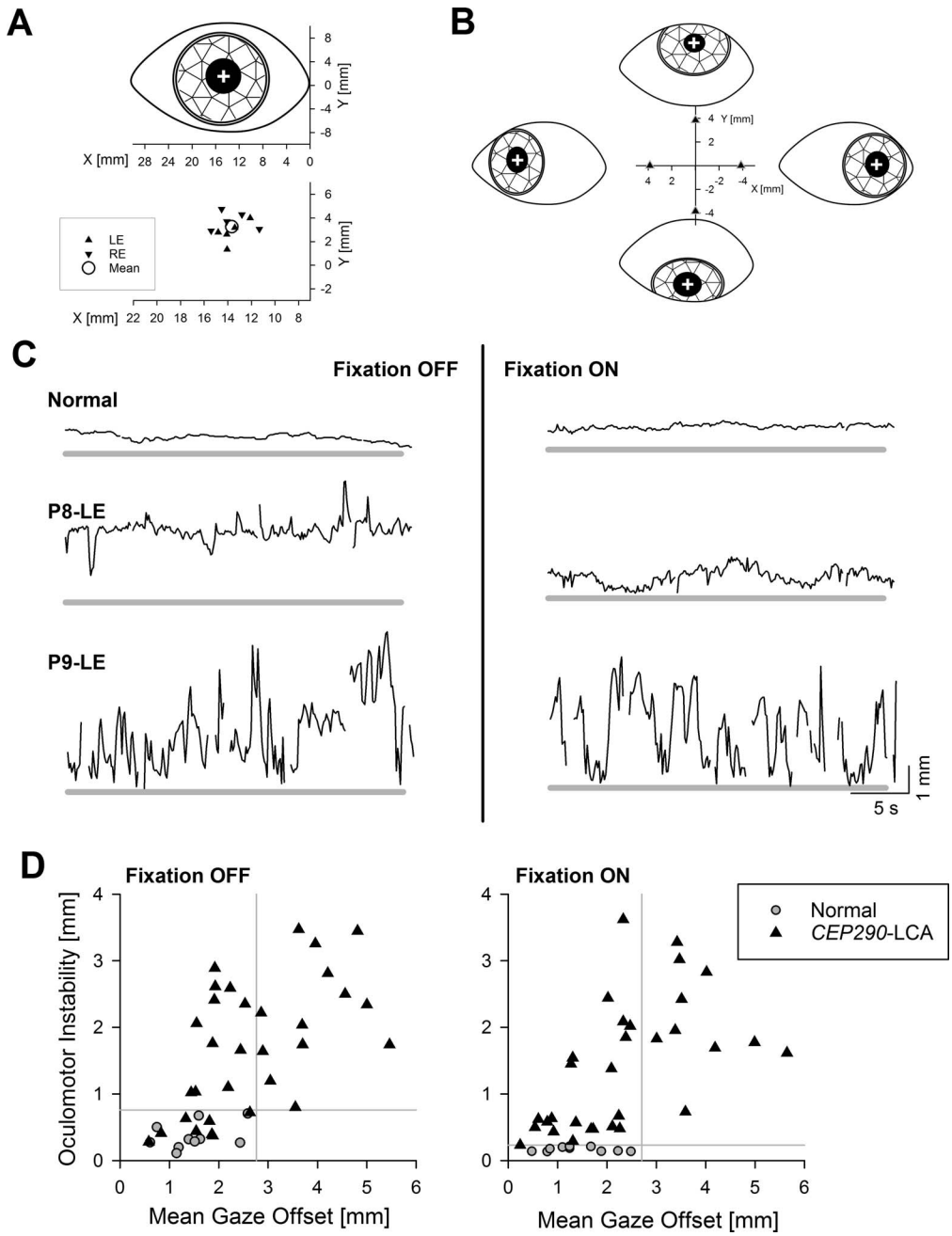

Figure 2. Spectrum of oculomotor features in *CEP290*-LCA. (**A**) *Upper*: Schematic representation of the coordinate system centered at the medial (nasal) canthus and the center of pupil (*white cross*) at primary gaze. *Lower*: Individual data from left (LE) and right (RE) eyes of all normal subjects at primary gaze. Mean value is also shown (*circle*). (**B**) Schematic representation of eyes fixating 30° eccentric along the four cardinal directions, and relative offsets of the center of pupil measured from the primary gaze locus. (**C**) Chart records showing the radial offset of the center of pupil from the mean normal primary gaze locus (*thick gray line*) during a 30-second-long recording epoch in a representative normal subject and two *CEP290*-LCA eyes. Two records shown are with (*right column*) and without (*left column*) fixation. (**D**) Oculomotor instability plotted against mean gaze offset in individual *CEP290*-LCA eyes (*triangles*; $n = 32$ eyes of 16 patients) recorded with and without fixation. Equivalent results from normal eyes are also shown (*gray circles*). *Gray lines* demarcate the upper (mean + 2 SD) limits of normal for each parameter. Reprinted with permission from Jacobson SG, Cideciyan AV, Sumaroka A, et al. Outcome measures for clinical trials of Leber congenital amaurosis caused by the intronic mutation in the *CEP290* gene. *Invest Ophthalmol Vis Sci*. 2017;58:2609–2622. © 2017 The Authors. Published by ARVO.

note that the cellular constituents of the ONL change with eccentricity from the fovea. The normal foveola, referring to the ~1° diameter center of the fovea, consists of only cone photoreceptors whereas the extrafoveal retina is mostly rods. The great majority of *CEP290*-LCA patients retain a substantial ONL in the central macular region that thins with eccentricity. The UHR SDOCT from a 10-year-old *CEP290*-LCA patient with bare light perception vision illustrates a typical scan (Fig. 3A, lower). The ONL has normal thickness at the cone-rich foveola, which suggests near-normal density of cone photoreceptor nuclei. Between the fovea and ~6° eccentricity, the ONL thins steeply and asymptotes to a very thin (~10 μm) layer with detectable outer plexiform layer (OPL) and external limiting membrane (ELM) boundaries. This layer likely represents a

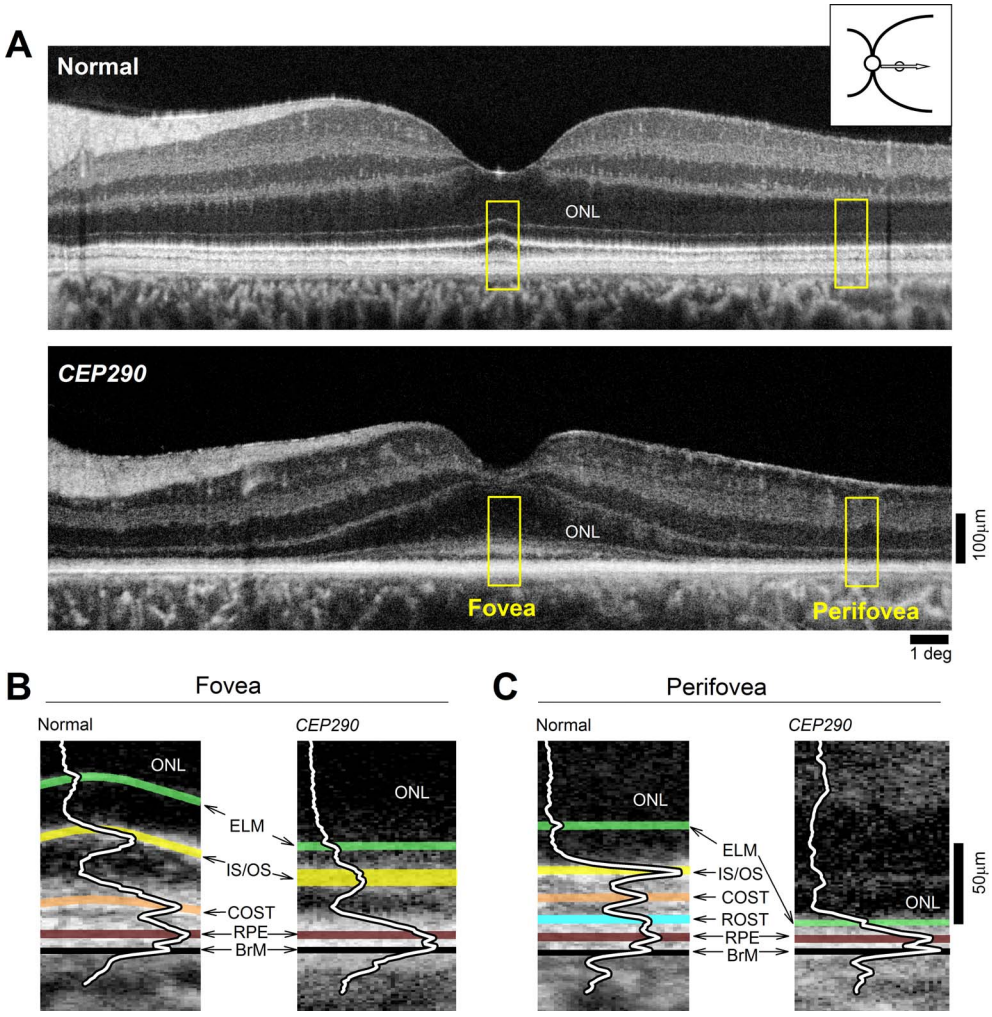

Figure 3. Retained photoreceptor nuclei with abnormal segments in *CEP290*-LCA. (**A**) OCT scans along the horizontal meridian through the fovea in a normal subject, and a *CEP290*-LCA patient. Images were obtained with a clinical ultrahigh resolution SDOCT system (Bi-µ; Kowa Company, Ltd.). Hyposcattering layer corresponding to the ONL is shown. *Inset upper right* shows location of scan. *Yellow boxes* outline foveal and perifoveal regions shown in (**B**, **C**). (**B**, **C**) Magnified views of the outer retina at foveal and temporal perifoveal locations demonstrating differences in the layers distal to the ONL. Overlaid are the longitudinal reflectivity profiles (LRPs). Hyperscattering signals highlighted as follows: *green*, ELM; *yellow*, IS/OS, near the junction of inner and outer segments; *orange*, COST, near the interface of cone outer segment tips and RPE contact cylinder (also called the interdigitation zone); *cyan*, ROST, near the interface between rod outer segment tips and RPE apical processes; *brown*, RPE, near the RPE cell bodies; and *black*, BrM, Bruch membrane. Figure courtesy of Alexander Sumaroka (Scheie Eye Institute, University of Pennsylvania).

single row of cone nuclei and lacking all rod nuclei.[39] Existence of normal foveal photoreceptors despite severe reduction of vision suggests a major dissociation of function and structure reminiscent of the *RPE65* form of LCA.[16] Quantitative comparison of light sensitivity and retinal structure in *CEP290*-LCA patients has provided direct evidence of the dissociation.[43]

Retained outer retinal photoreceptor nuclei are necessary but not sufficient to drive retinal visual function: Also needed are outer segments for phototransduction and inner segments for energy production. Magnified OCT images show at least four foveal and at least five extrafoveal hyperscattering peaks distal to the ELM where inner and outer segments and RPE processes would be expected to reside in normal eyes (Figs. 3B, 3C). These hyperscattering signals are thought to originate from histologic layers near the junction between inner and outer segments (IS/OS, also called inner segment ellipsoid zone), near the interface between cone outer segment (COS) tips and RPE contact cylinder (also called the interdigitation zone, IZ), near the interface between rod outer segment tips (ROST) and RPE apical processes, near the RPE cell bodies, and at the Bruch membrane (BrM).[67–71] Of note, distinct ROST, RPE, and BrM peaks apparent in normal extrafoveal scans (Fig. 3C, left) are often amalgamated into a single peak in lower-resolution clinical images.[72]

At the *CEP290*-LCA fovea, the ELM to BrM distance is approximately half of normal and lacks the normal layering (Fig. 3B). There can be a hyperscattering layer likely corresponding to a widened IS/OS peak with substantially shortened distance to the ELM suggesting shortened inner segment lengths. Instead of a hyperscattering COS tips (COST) peak, *CEP290*-LCA foveas have a wide hyposcattering layer that likely corresponds to misshapen OS or OS debris or both. In the perifoveal region, there are detectable OPL and ELM signals suggesting a retained ONL layer that is less than one-third the normal thickness. IS/OS, ROST, and COST peaks are not detectable in perifoveal scans of *CEP290*-LCA (Fig. 3C).

Investigative Ophthalmology & Visual Science

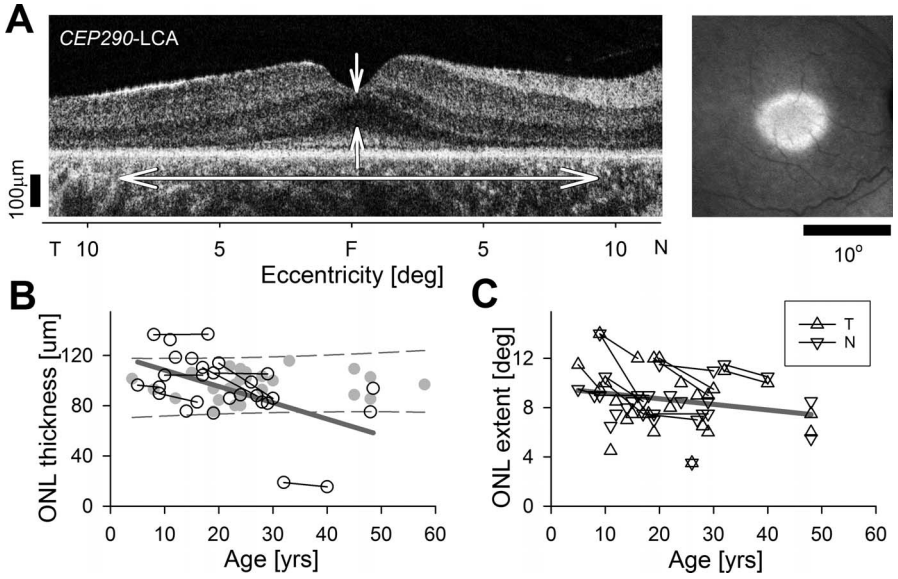

Figure 4. Slow rate of cone photoreceptor degeneration in *CEP290*-LCA. (**A**) Horizontal OCT from a *CEP290*-LCA patient (*left*) demonstrating the foveal ONL thickness and ONL extent measures. Near-infrared autofluorescence imaging (*right*) demonstrating preserved central macular region of RPE melanization. (**B**, **C**) Quantitation of foveal ONL thickness (**B**), and ONL extent from fovea in nasal and temporal directions (**C**) in a group of *CEP290*-LCA patients evaluated cross-sectionally at different ages. Also shown are a subset of patients with longitudinal data (*connected symbols*). Linear regressions (*thick gray line*) fit to all data. Redrawn from data in Jacobson SG, Cideciyan AV, Sumaroka A, et al. Outcome measures for clinical trials of Leber congenital amaurosis caused by the intronic mutation in the *CEP290* gene. *Invest Ophthalmol Vis Sci*. 2017;58:2609–2622. © 2017 The Authors. Published by ARVO.

Disease Progression

Previously we showed that rod photoreceptors develop in *CEP290*-LCA but rapidly degenerate postnatally with some patients retaining midperipheral rods in the first decade of life.[39] By the second decade of life, most patients retain central cones devoid of rods. Considering the longstanding hypothesis that cones require rod-derived viability factors for their survival,[73] we recently estimated the rate of degeneration of cone photoreceptors in *CEP290*-LCA.[35] OCTs from 20 patients across five decades of life were quantified cross-sectionally. In a subset of seven patients, longitudinal recordings performed over nearly a decade were analyzed. The ONL thickness at the fovea was normal or hypernormal in all patients but one (Fig. 4B). Longitudinally there were either no detectable changes or there was some mild thinning. Combining the cross-sectional and longitudinal results, and accounting for the patient with foveal degeneration, foveal ONL thickness tended to decrease at an average rate of 1.3 µm/year (Fig. 4B, gray regression line). When the patient with foveal degeneration was excluded, the average rate of foveal ONL loss was 0.7 µm/year.

The elliptical region of central macular preservation in *CEP290*-LCA slowly constricts over time, and this is demonstrated by quantifying the nasal and temporal extents of ONL retention (Fig. 4C). Analysis of the central elliptical region extent of melanized RPE with near-infrared reduced illuminance autofluorescence imaging (NIR-RAFI) showed a similar slow constriction over decades.[35] These results suggest a very wide window over which the dysfunctional *CEP290*-mutant cones are amenable to vision improvement treatments. However, evaluation of changes to natural history of disease would be expected to be challenging.

Postreceptoral Structure Along the Retinocortical Pathway

Connectivity between the outer retina and the visual cortex is necessary for patients to perceive the consequences of efficacious treatment of their cone photoreceptors. To understand whether the pathways are available to signal photoreceptor signals to higher vision centers, we evaluated proximal structures. Within the retina, cells immediately postsynaptic to photoreceptors are located in the inner nuclear layer (INL), which had normal or hypernormal thickness (Figs. 5A, 5B). Tertiary neurons are located in the ganglion cell layer (GCL), which also had normal or hypernormal thickness (Figs. 5A, 5B). Axons of ganglion cells are located in the retinal nerve fiber layer (RNFL), which was also normal or hypernormal in thickness (Figs. 5A, 5B). Thickening of inner retinal layers is thought to represent retinal remodeling[38] and was most prominent in the perifoveal retinal areas of *CEP290*-LCA with little evidence of photoreceptors remaining. The central region with the retained cone photoreceptors tended to have normal or near-normal inner retinal structure.

What about postretinal structures? In two patients with *CEP290*-LCA, we had the opportunity to make measurements. Interpial optic nerve diameters were normal (Fig. 5C), and whole-brain morphometric analysis found no significant deviations from normal cortical or subcortical anatomy (Fig. 5D). Retinal and postretinal anatomy taken together (Figs. 3–5) allows us to conclude that central macular cone photoreceptors in *CEP290*-LCA retain sufficient pathways to potentially carry vision signals from cone photoreceptors to the visual cortex upon administration of a successful therapy.

Function of Postreceptoral Circuits in Patients Lacking Perception

A large subset of *CEP290*-LCA demonstrates severe (often congenital) lack of visual perception. Prerequisites to any treatment approaches in these patients must include evidence that the retained postreceptoral structures (described above) demonstrate function. For this, we took advantage of the

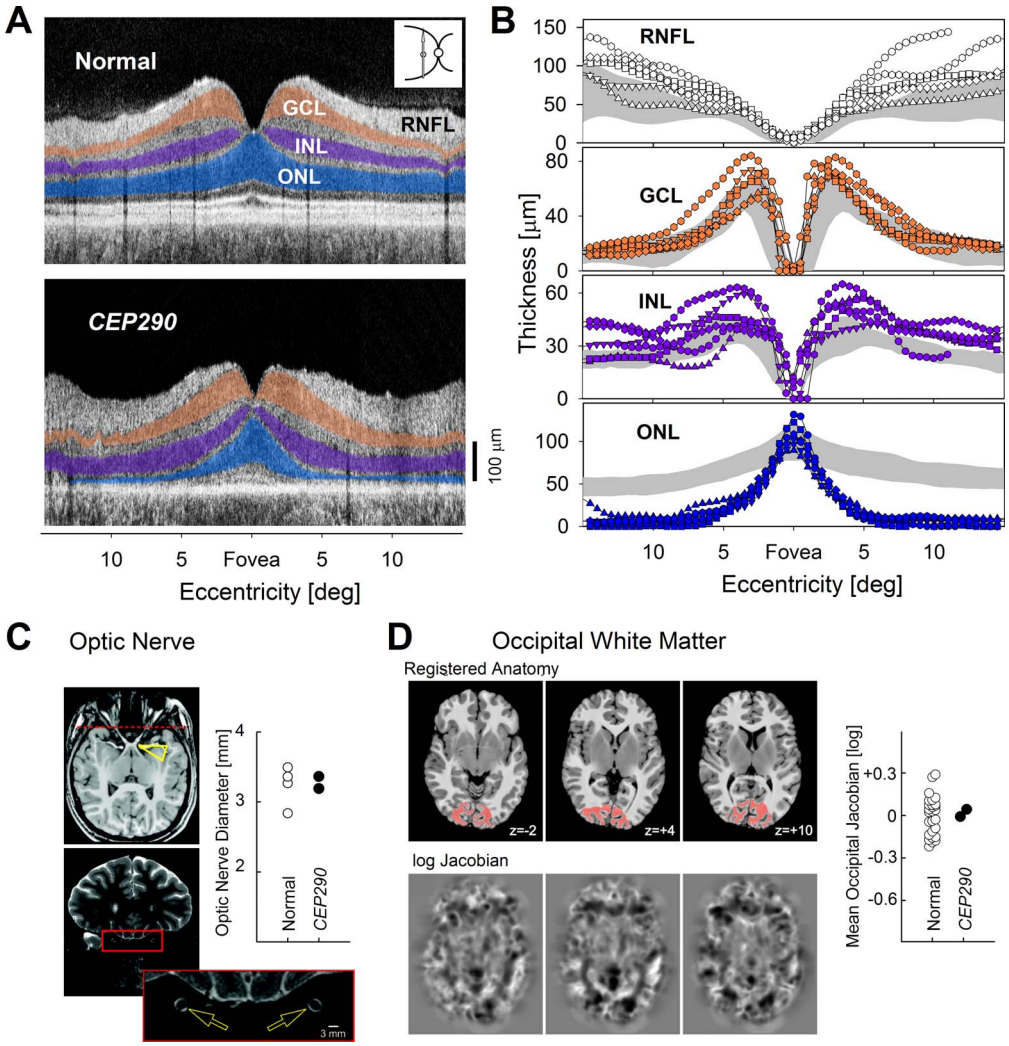

Figure 5. Postreceptoral structures along the retinocortical pathway in *CEP290*-LCA. (**A**) *Left*, OCT scans along the vertical meridian in a normal subject and a *CEP290*-LCA patient. ONL is highlighted *blue*, INL is highlighted *purple*, and GCL is highlighted *orange*. (**B**) Quantitation of the three nuclear layer and the RNFL thickness in 6 *CEP290*-LCA patients compared with normal results (*shaded areas*; mean ± 2 SD). (**C**) Optic nerve anatomy. A normal-appearing optic chiasm (*arrowhead*) observed on T1 imaging. High-resolution T2-weighted axial and coronal images were obtained through the optic nerves. The position of the coronal slice displayed is indicated by the *dashed line* on the axial image. The cross-sectional diameter of the interpial optic nerve (*arrows*) was estimated at three positions along each nerve, and the average diameter is within the range of normal (plot). (**D**) Whole-brain morphometric analysis. The T1-weighted anatomic images from *CEP290*-LCA and controls were warped to a representative template (*top row*). The (log) determinant of the Jacobian matrix calculated during warping for each subject (*bottom row*) indexes the degree to which cerebral tissue is smaller or larger than the template image. No significant deviation from control measures was seen in two *CEP290*-LCA patients. A focused analysis was conducted within occipital lobe white matter (red on the registered anatomy). The z-position (mm) of each axial slice relative to the anterior commissure is indicated. The average (log) Jacobian measure within the occipital white matter for *CEP290*-LCA and normal subjects indicates no differences (plot). (**C**, **D**) Reprinted with permission from Cideciyan AV, Aleman TS, Jacobson SG, et al. Centrosomal-ciliary gene *CEP290/NPHP6* mutations result in blindness with unexpected sparing of photoreceptors and visual brain: implications for therapy of Leber congenital amaurosis. *Hum Mutat*. 2007;28:1074–1083. © 2007 John Wiley & Sons, Inc. Published by Wiley-Liss, Inc.

pupillary light reflex (PLR). PLR is normally driven by a combination of four outer retinal photoreceptors and by melanopsin-containing intrinsically photosensitive retinal ganglion cells (ipRGCs) depending on the stimulus used, adaptation conditions, and ambient light levels.[74,75] When outer retinal photoreceptors are genetically, pharmacologically, or spectrally silenced, PLR is dominated by the ipRGC function (Fig. 6). Using standard stimuli, many *CEP290*-LCA patients show no detectable PLR (Figs. 6A–C). However, higher stimulus strengths allow recording of robust signals (Figs. 6D, 6E), which suggest that at least some postreceptoral circuits are functional. Whether this functionality extends to the visual cortex in patients with congenital lack of vision remains to be determined.

Treatment Approaches to *CEP290*-LCA

The most promising approaches to treating monogenic IRDs to date are gene augmentation therapies using AAV vectors.[25,76] However, the full-length *CEP290* gene is too large for the AAV capacity and thus alternative avenues are required for the treatment of *CEP290*-LCA. Alternatives include gene editing,[77,78] augmentation with gene fragments,[79–81] lentiviral vectors with larger packaging capacity,[82] or splitting the transgene across two separate AAV vectors.[83] Antisense gene

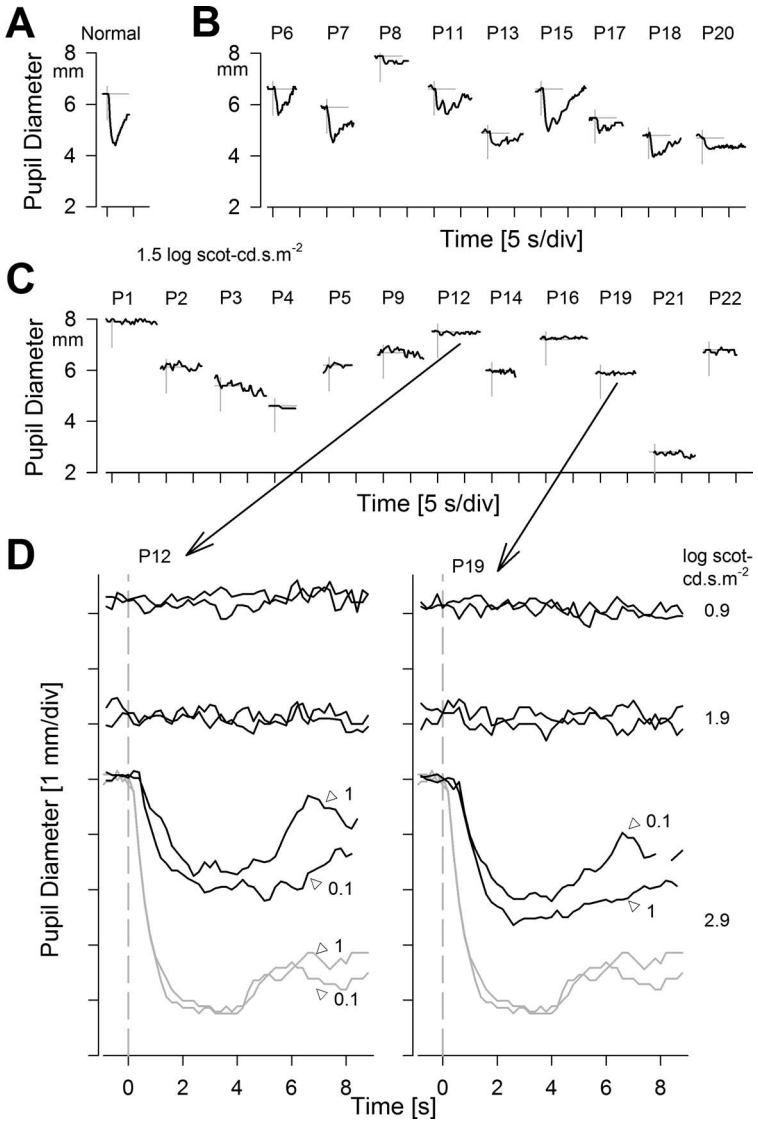

Figure 6. Pupillary light reflexes in *CEP290*-LCA. (**A–C**) Dynamics of pupil constriction in the dark to a 0.1-second-duration achromatic bright standard stimulus (1.5 log scot-cd.s.m^{-2}) in a representative normal (**A**), *CEP290*-LCA patients grouped into those with detectable responses (**B**), and those without (**C**). (**A–C**) Modified from Jacobson SG, Cideciyan AV, Sumaroka A, et al. Outcome measures for clinical trials of Leber congenital amaurosis caused by the intronic mutation in the *CEP290* gene. *Invest Ophthalmol Vis Sci*. 2017;58:2609–2622. © 2017 The Authors. Published by ARVO. (**D**) Use of higher stimulus luminance range in two of the eyes with no pupillary response to standard stimuli. Notably, 0.9 and 1.9 log scot-cd.s.m^{-2} stimuli do not evoke responses, whereas 2.9 log scot-cd.s.m^{-2} stimuli evoke definite responses that are smaller and slower than normal. Similarity of responses with 0.1- and 1-second-long stimuli suggests reciprocity between stimulus luminance and duration. (**D**) Modified from Charng J, Jacobson SG, Heon E, et al. Pupillary light reflexes in severe photoreceptor blindness isolate the melanopic component of intrinsically photosensitive retinal ganglion cells. *Invest Ophthalmol Vis Sci*. 2017;58:3215–3224. © 2017 The Authors. Published by ARVO.

therapy is a promising therapeutic approach that takes advantage of a frequently occurring intronic mutation (c.2991+1655A>G) that creates a splice donor site that permits a cryptic exon insertion and leads to premature termination of protein synthesis.[55] Antisense RNA oligonucleotides (AONs, or ASOs) are designed to target the pseudoexon region to increase normal protein expression.[84–86] A phase I/IIa clinical trial with such an AON is ongoing, and the current authors are investigators at one of the sites of this trial (NCT03140969 Clinicaltrials.gov). Preliminary results support an acceptable safety profile and a potential for improvement of visual acuity and light sensitivity.[87]

GUCY2D-LCA

Phototransduction and LCA1

Phototransduction abnormalities have long been associated with IRDs,[88] and mutations in genes encoding phototransduction proteins are now known causes of inherited retinal dysfunction and degeneration.[1,2,89] The gene *GUCY2D* encodes retinal guanylyl cyclase (retGC1), which modulates phototransduction in rods and cones. RetGC1 is expressed in both cones and rods as a 120-kDa membrane protein that is responsible for the resynthesis of cyclic guanosine monophosphate (cGMP) required for the recovery of the dark-adapted state of photoreceptors after phototransduction (Fig. 7).

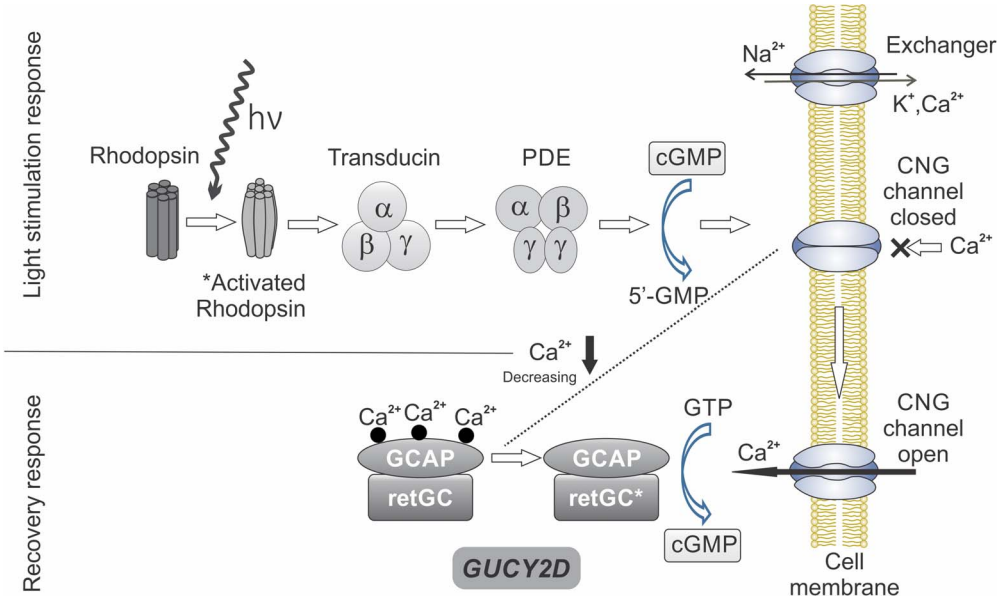

Figure 7. Phototransduction and *GUCY2D*. Absorption of light by rhodopsin in the rod photoreceptor outer segment activates rhodopsin and starts the cascade of reactions that successively include activation of transducin and cGMP phosphodiesterase (PDE), which hydrolyzes cGMP. Reduction in the concentration of cGMP leads to closure of cGMP-gated channels (CNG). The recovery response occurs as there is continued decrease of intracellular Ca^{2+} and activation of guanylyl cyclase (retGC) by GCAP (guanylyl cyclase activating protein). This replenishes cGMP and causes reopening of CNG. *GUCY2D*, the gene encoding retGC, is key to response recovery. Redrawn and reprinted with permission from Boye SE. Insights gained from gene therapy in animal models of retGC1 deficiency. *Front Mol Neurosci*. 2014:7:43. © 2014 Boye.

Autosomal recessive mutations in *GUCY2D* lead to LCA1[90] likely due to dysregulation of guanylyl cyclase causing an equivalent state to chronic light exposure of photoreceptors.[91]

Visual Consequences

Visual function of *GUCY2D*-LCA is severely abnormal.[92] All patients have nystagmus with visual impairment noted in the first year of life. Ophthalmoscopic findings include retinal vessel attenuation and a granular appearance to the peripheral fundus; macular pigmentary disturbances have been observed. Visual acuity is abnormal and ranges from 20/80 to no light perception; the level of acuity is not related to age.[44,92] Using acuity as a qualitative severity estimate, 50% of the *GUCY2D*-LCA patients in our cohort had CF or worse in the best-seeing eye[44] compared with 62% to 89% of *CEP290*-LCA and 10% of RPE65-LCA. Like *CEP290*-LCA, the *GUCY2D*-LCA patients were also hyperopic. Visual fields by kinetic perimetry can be detectable in some patients, but these are small central islands and there are occasional peripheral islands with the largest and brightest target (V-4e). Most patients have nondetectable rod and cone electroretinograms (ERGs) but up to 25% can show very reduced rod ERG signals.[44,92]

Cone and rod sensitivities were measurable with FST in almost all patients in our cohort (Fig. 8). Both photoreceptor-mediated sensitivities showed a range of results (Fig. 8A). Highest cone sensitivities could be as little as 1 log unit reduced from mean normal. Unlike in *CEP290*-LCA, rod sensitivity was detectable in all but a few patients. By FST, rod sensitivities can be near normal but the range was wide, and there were also those with minimally or no detectable rod function. Notable in the cone and rod sensitivities displayed from highest to lowest (Fig. 8A) is the fact that the patients with the best cone sensitivities are not the same as those with the highest rod sensitivities. The relationship of rod and cone sensitivity in each patient can be complex.[44]

Cone vision was related to measurable visual acuity (Fig. 8B); cone sensitivity losses (CSL) ranged from 1.0 to 4.7 (median 2.8) log units. Rod sensitivity losses (RSL) ranged from 0.1 to 6.5 (median 1.4) log units. Side-by-side comparison of cone and rod sensitivity losses shows that many of those patients with low acuity and considerable cone sensitivity losses could have substantial rod sensitivity by FST and vice versa (Fig. 8B). We asked whether there was a way to group patients by cone and rod vision impairment. The answer was that there may be different groups of patients: There were two small groups and a larger third group that included most of the patients.[44] The two small groups shared severe rod vision disturbances but differed in that one group had <2 log units of cone vision abnormality and the other had severe cone dysfunction. The remainder of the patients had less severe rod loss and a spectrum of cone losses, and the cone and rod sensitivity losses were moderately related.[44] Substantial rod function is thus measurable by full-field psychophysics in *GUCY2D*-LCA patients; there was no clear relationship of patient age to presence of residual rod function. The presence of considerable psychophysically measured rod function was confirmed objectively in some patients by ERG.[92]

Photoreceptor Structure

Despite the major losses of photoreceptor function, LCA patients with *GUCY2D* mutations present with a mainly intact retina morphologically and there are retained rods and cones in both the macula and peripheral retina into adulthood.[44,92] More specifically, we first reported that photoreceptor ONL thickness by OCT was within normal limits except in the foveal region of some patients.[92] The foveal region was studied, and whereas 50% of the patients can have foveal ONL that is within normal limits, almost all show abnormalities in more distal retinal elements. The foveal bulge (FB) or bowing, attributed to increased COS length at this locus in normal subjects, is less evident or not present in most of the *GUCY2D*-LCA patient scans (Fig. 9A, left). The IS/OS reflectivity in the patient scans appears thickened and less intense. When we quantified the FB in normal subjects ($n = 10$, ages 8–62), the mean FB was 16.08

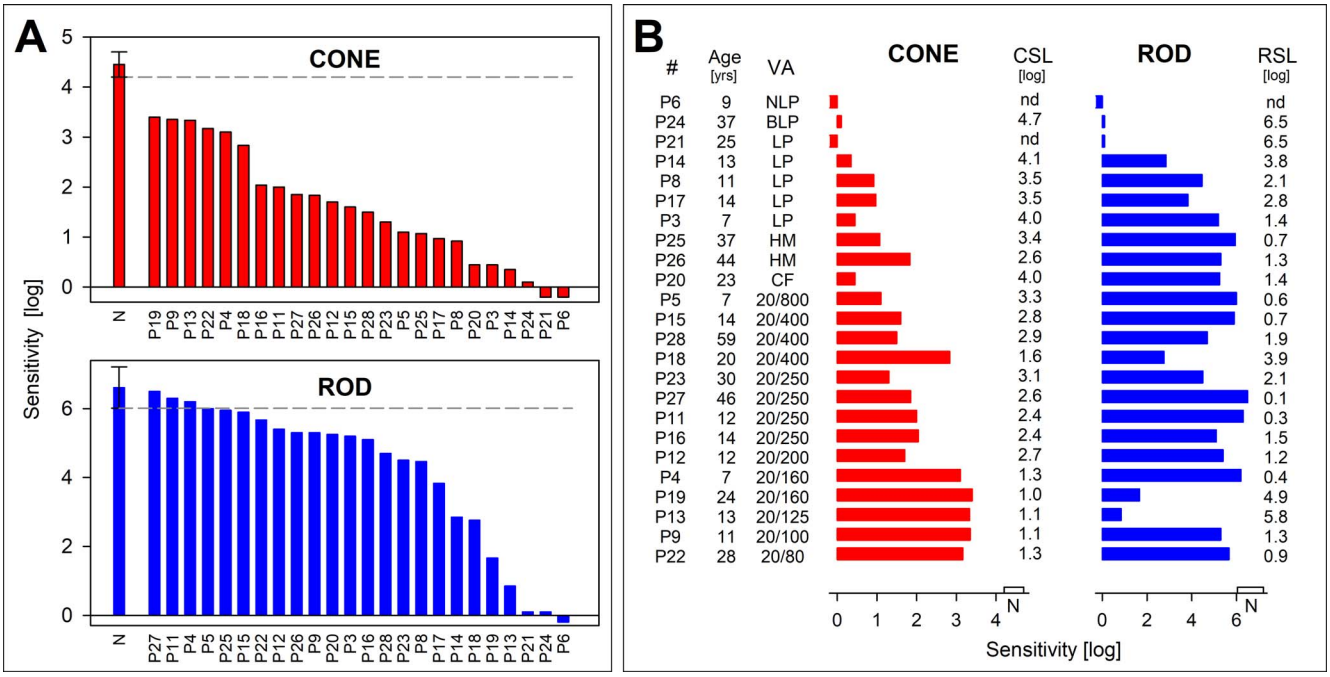

Figure 8. Rod and cone photoreceptor-mediated function in *GUCY2D*-LCA. Full-field sensitivities for light-adapted red (*red bars*) and dark-adapted blue flashes (*blue bars*) to assess cone and rod function, respectively. (**A**) Sensitivities are ranked from high to low to illustrate the range of dysfunction in *GUCY2D*-LCA patients. All cone sensitivities are abnormal by 1 log unit or more, and the range includes very severe dysfunction. Rod sensitivities could reach normal levels in some patients, and there can be relatively good rod function in the majority of patients. Note that patient order (horizontal axis in each graph) is not the same for both rod and cone sensitivity levels, indicating that patients with better cone function are not necessarily the same as those with better rod function. (**B**) Cone and rod function ranked by visual acuity (lowest to highest, top to bottom). There is a strong relationship between acuity and the cone metrics, but rod and cone sensitivity are not closely related, as mentioned in (**A**). NLP, no light perception; BLP, bare light perception; LP, light perception; HM, hand motions; CF, count fingers; nd, not detected. Negative-going bars indicate no perception of the stimuli. Rod sensitivity for patient 21 and patient 24 and cone sensitivity for patient 24 were very close to instrument limit; these bars were set to 0.1 for this depiction. *Brackets* on (**A**) and *bars* on the horizontal axes on (**B**) are centered on the normal (N) mean sensitivity and the limits represent ±2 SD. Figure courtesy of Alejandro J. Roman (Scheie Eye Institute, University of Pennsylvania).

μm ± 3.18 (mean ± standard deviation, SD). In *GUCY2D*-LCA patients, mean FB was 4.42 μm ± 5.43. The difference in FB between the two groups was statistically significant ($P \leq 0.001$, *t*-test). Only approximately 15% of the patient scans had a FB within 2 SD of the normal mean.[44]

Further measurements of the foveal outer retina suggested a disturbance of COS tips as they interdigitate with the RPE processes. For example, the magnified and colorized images of two *GUCY2D*-LCA patients are compared with the scan of a normal subject (Fig. 9A, right). One patient illustrates slightly reduced foveal ONL and a lack of FB attributable to COS thinning. The other patient has definitely reduced foveal ONL and a central region in which the COS layer appears to be lost; this could be an early manifestation of a hyporeflective zone such as previously described in other maculopathies. COS thickness was reduced in approximately 85% of patients. In the remainder, the normal reflective landmarks were not present. We also compared the intensity of the inner segment/outer segment (IS/OS) band to the intensity of the deeper complex of reflections composed of COST and RPE to calculate a relative intensity ratio of IS/OS to RPE. The relative intensity in the group of normal subjects ranged from 0.6 to 0.94, whereas in *GUCY2D*-LCA patients with a detectable IS/OS band, the relative intensity ranged from 0.36 to 0.76. Fifty percent of the patients had a relative intensity that fell within the narrow interval of 0.5 to 0.6. There was a statistically significant difference in relative intensity of IS/OS between the control group and *GUCY2D*-LCA patients.[44]

The *GUCY2D*-LCA patients had considerable variation of rod function from nearly normal to severely abnormal (Fig. 8). Were there any abnormalities of rod photoreceptor retinal structure? We studied the "rod hotspot" (RHS), the superior retinal region of highest rod density in the human eye (Fig. 9B). The ONL was within normal limits in all but one of the patients. When comparing the mean ONL results of normal control subjects at the RHS and that of *GUCY2D*-LCA patients, there was no statistically significant difference between these two groups. There was also no dramatic loss of thickness of the laminae distal to the ONL; only one patient had rod outer segment (ROS) thickness that was below the normal limits. A detailed examination of the scans revealed that the relative intensity of the IS/OS (by comparison with the intensity of the deeper complex of reflections) was reduced.[44]

The key issue of structure versus function (and the potential for improvement in vision) was quantified in the fovea of those *GUCY2D*-LCA patients with measurable COS length and definable cone function.[44] We asked if the relationship of cone function to cone structure in *GUCY2D*-LCA was behaving like a pure photoreceptor degeneration. Loss of photoreceptor structure is typically the underlying basis for loss of photoreceptor function. In *GUCY2D*-LCA patients with measurable foveal ONL and COS, we plotted structure versus cone function and compared results to those of normal subjects and other IRDs, specifically RP (Fig. 10A). We defined structure as the product of ONL thickness (a proxy for photoreceptor numbers) and COS length (a proxy for opsin molecules within each retained photoreceptor) at the fovea. Cone sensitivity loss was used as a measure of visual function. We plotted the structure–function data from different forms of RP and applied a simple linear model that has been used to

Investigative Ophthalmology & Visual Science

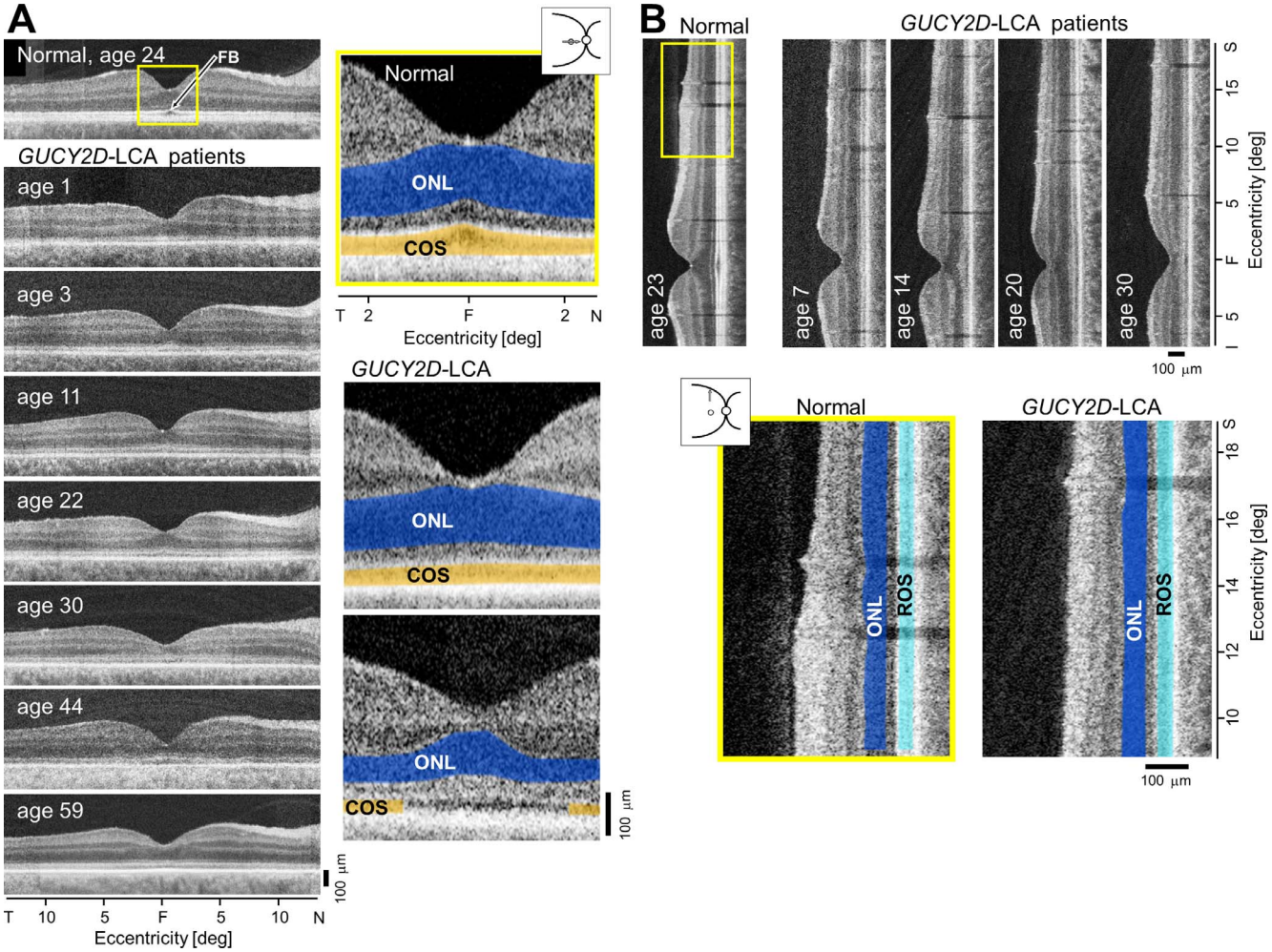

Figure 9. Retinal structure at the fovea and perifovea in *GUCY2D*-LCA. (**A**) Cross-sectional OCT scans along the horizontal meridian through the fovea (F) in a normal subject and seven *GUCY2D*-LCA patients, ranging in age from 1 to 59 years. Enlarged central scans (*yellow box*) in a normal subject and two *GUCY2D*-LCA patients are also shown. The ONL is highlighted in *blue* and the COS layer is in *orange*. The *upper* image from a patient illustrates a thinned COS layer but normal ONL. The *lower* image is from a patient with reduced ONL thickness and an interrupted COS layer, suggesting a central absence of COS. FB, foveal bulge. (**B**) OCT scans along the vertical meridian including the fovea and continuing into the superior perifoveal region in a normal subject and four patients with *GUCY2D*-LCA ranging in age from 7 to 30 years. Enlarged scans (*yellow box*) in a normal subject and a patient showing comparable ONL (*blue*) and rod outer segment layer (*light blue*) thickness. Figure courtesy of Alexander Sumaroka (Scheie Eye Institute, University of Pennsylvania).

describe this relationship in various retinal degenerations. The results indicate that the other RP genotypes were behaving similarly: Visual sensitivity was reduced linearly with quantum catch. Most of the *GUCY2D*-LCA patient data, however, differed from the other genotypes and fell outside of the 95% confidence interval of normal variability. The current results support the observation that in most *GUCY2D*-LCA patients there is a greater degree of dysfunction than could be explained by the structural loss of cone nuclei and shortening of COS.

As with cone structure and function, we asked if the rod dysfunction in relation to rod structure in *GUCY2D*-LCA was behaving like a pure photoreceptor degeneration. All but one *GUCY2D*-LCA patient showed a relationship that fell outside of the predicted model for a pure photoreceptor degeneration (Fig. 10B). There was disproportionate loss of rod function for the remaining rod structure.

Disease Progression

To date there is no published natural history of the retinal disease in *GUCY2D*-LCA. Investigators with quantitative structural and functional data in *GUCY2D*-LCA patients should consider performing such a study. A simple route to such data would be to perform follow-up evaluations on recent examinations (i.e., those with modern LCA-specific methods) that included potential outcomes for a clinical trial such as OCT (with segmentation and attention to outer retinal laminae), FST (dark- and light-adapted conditions with chromatic stimuli to capture rod and cone function), pupillary light responses, and oculomotor instability (OCI) in addition to conventional techniques such as visual acuity but with consideration of low-vision methods such as the Berkley Rudimentary Vision Test.

Postreceptoral Structure Along the Retinocortical Pathway

An appropriate concern to be addressed in pretreatment studies is whether the severe visual impairments resulting from congenital retinal dysfunction in *GUCY2D*-LCA may alter the structure and function of the brain of these individuals and thereby prevent therapeutic efficacy. We thus studied the

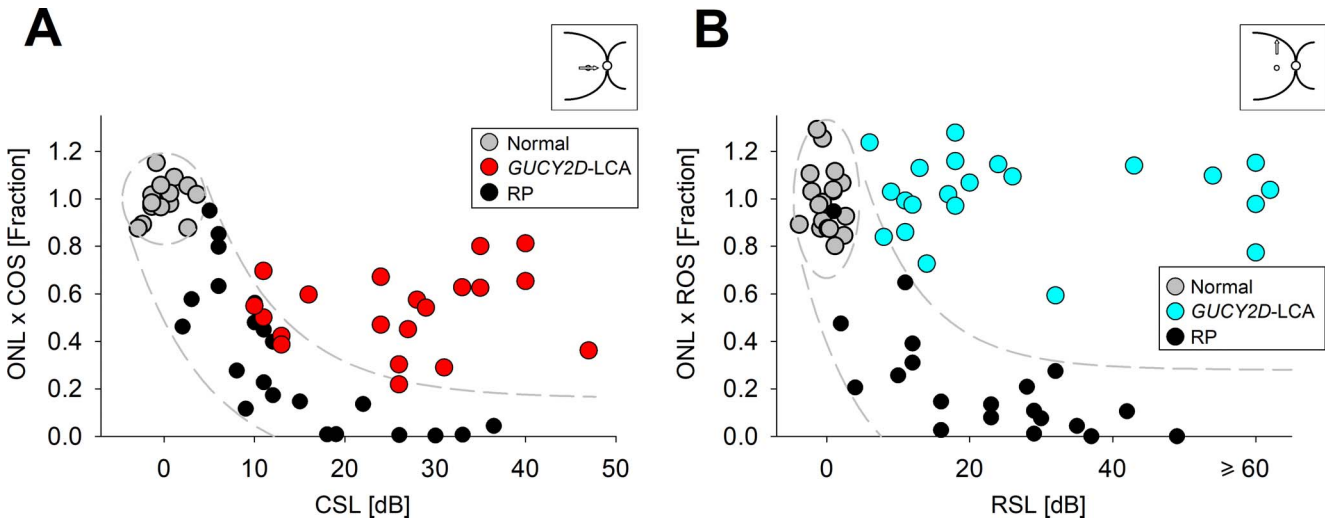

Figure 10. Relation of retinal structure and visual function in *GUCY2D*-LCA. (**A**) Relationship between product of foveal ONL and COS thickness (as a fraction of normal mean) and visual function (cone sensitivity loss, CSL) in *GUCY2D*-LCA patients (*red*), normal control subjects (*gray*), and patients with forms of autosomal recessive retinitis pigmentosa, RP (*black*). CSL is estimated from FST in *GUCY2D*-LCA and foveal cone perimetry in other patients and normal subjects. (**B**) Relationship between product of rod hotspot ONL and ROS thickness (as a fraction of normal mean) and visual function (rod sensitivity loss, RSL) in *GUCY2D*-LCA patients (*blue*), normal control subjects (*gray*), and patients with various forms of RP (*black*). RSL is estimated from FST in *GUCY2D*-LCA and from dark-adapted perimetry in other patients and normal subjects. The ellipses in (**A**, **B**) enclose the 95% confidence interval of bivariate Gaussian distributions, indicating the regions of normal variability. Translating the normal variability along an idealized model for pure photoreceptor degenerations produced a region of uncertainty, which is shown as the areas bound by the *dashed lines*. Figure courtesy of Alexander Sumaroka and Alejandro J. Roman (Scheie Eye Institute, University of Pennsylvania).

postretinal visual pathways in six molecularly defined *GUCY2D*-LCA patients using multimodal magnetic resonance imaging (MRI) of the brain.[93] The patients had visual acuities ranging from 20/160 to no light perception, and all patients had the characteristic findings of severe visual impairment but relatively preserved retinal structure. As expected, the visual loss in *GUCY2D*-LCA was accompanied by attenuation and constriction of the cortical response. Comparisons were made with normally sighted subjects and other congenitally "blind" subjects with causation that disrupted retinal structure. *GUCY2D*-LCA patients showed no difference in size of the optic chiasm from normal, and this was consistent with our measurements of retinal GCL thickness by OCT. Blind subjects with other etiologies of disease were significantly different; that is, the optic chiasm was smaller. Along the visual pathways through the lateral geniculate nucleus and pericalcarine white matter, the *GUCY2D*-LCA results were intermediate between normal and "other blind" subjects but not significantly different from either group. Like "other blind" subjects, the *GUCY2D*-LCA patients had thickened visual cortex gray matter, which is consistent with early and severe deprivation of form vision.[93] Although there remain many questions about the relation of pretreatment brain measures to posttreatment visual recovery prospects in *GUCY2D*-LCA, results to date are sufficiently promising to continue on the path toward treating the retina of these patients.

Treatment Approaches to *GUCY2D*-LCA

Preclinical studies in multiple LCA1 murine models have established that using gene therapy to deliver the *GUCY2D* gene to the rods and cones of the eye using a recombinant AAV vector is feasible and efficacious.[94–99] Structural preservation and functional restoration of photoreceptors were achieved as demonstrated by histologic examinations, ERGs, and improvements in vision-elicited behavior. Furthermore, AAV-mediated gene replacement has proven safe and effective for the treatment of other retinal diseases, most notably *RPE65*-LCA.[20–24,26,29,31]

An early phase gene augmentation clinical trial for *GUCY2D*-LCA should primarily establish safety of the therapeutic agent (which would be delivered by the subretinal route) and secondarily determine if there is preliminary evidence of efficacy. A plan would be to treat a relatively large region of central retina involving not only the cone-rich fovea but also surrounding rod-rich retina. What parameters could be used to determine criteria for early and later cohorts and to monitor post treatment for efficacy? Beginning with functional criteria, it would seem judicious to include in the earlier cohorts patients with measurable but very reduced visual acuity, and CSL (by FST) between 2 and 4 log units (acuity equivalent of worse than 20/200 and including those with light perception vision). The considerable range of results for CSL as well as RSL in *GUCY2D*-LCA patients leads to the suggestion that earlier cohorts should also have substantial RSL (again, for example, between 2 and 4 log units). The hypothesis could then be tested that therapy may affect rod as well as cone function. Later cohorts could answer questions about the effects of therapy in those patients with relatively equal CSL but different degrees of RSL and those patients with the most profound CSL and RSL.

Structural abnormalities showed a gradient in *GUCY2D*-LCA patients but the gradient of function is far greater. FB and IS/OS intensity would be valuable to monitor for changes throughout a trial, but less valuable as criteria for defining cohorts to enter the trial. Patients with OCT revealing a pattern of severe central photoreceptor cellular loss could be relegated to later cohorts after it has been determined what the effects (negative and positive) are of therapy.

CONCLUSIONS

Patients with IRDs seek diagnoses, prognoses, and therapies from their doctors. Most ophthalmic practitioners are not specialized in such disorders, so the responses to the many questions posed depend on their previous training about these

rare diseases. The extensive amount of material to learn about treatable ophthalmic diseases makes IRDs (other than some of the characteristic funduscopic changes) one of the least emphasized topics during training. What do patients hear from their practitioners when an ophthalmic examination reveals some pigmentary retinopathy? They are usually told that their disease is incurable; that it leads to progressive blindness; and that it can be genetic (implying passed along to further generations). Most depressing to the affected patient is a frequent remark that further follow-up is not needed, suggesting that the case is hopeless and of no particular interest to that practitioner.

Times have changed, however, and now doctors can provide more information to IRD patients. The diagnosis can be defined not only clinically but also by molecular testing. The genetics in the family can become less of a guess and more certain. A literature of gene-specific natural history studies is growing, so questions about prognosis may be able to be answered. And even if the ophthalmic practitioner is not particularly interested in these rare diseases, patients can be guided to knowledge of their specific problem by referral to a growing number of IRD specialists. Accurate diagnostics at the clinical and molecular levels have led to clinical trials for a few of the IRDs. Given strong preclinical evidence for considering a clinical trial, pharmaceutical companies are becoming more interested in the concept. The goal of this manuscript is to point out that careful selection of diseases for treatment in the current era derives not only from understanding of the gene and the relevant disease models, but also from decisions about whether human vision can be potentially improved by intervention. The alternative (and more common) therapies that seek to delay the time course of visual deterioration need to be preceded by quantitative measures of the disease natural history. If not, the major effort, expense, and risk of some novel therapies may not be in the patient's best interest. Advances will continue, and despite the understandable desperation of a patient for some form of therapy, the ophthalmic practitioner should be sufficiently educated in relevant progress to provide up-to-date and accurate counsel.

Acknowledgments

The authors thank current and previous members of their laboratories, particularly Alexander Sumaroka, Malgorzata Swider, Alejandro J. Roman, Jason Charng, Alexandra V. Garafalo, Arun K. Krishnan, Brianna Lisi, Evelyn P. Semenov, Rebecca Sheplock, Christian A. Powers, Valeryia Aksianiuk, and Robert Russell for their participation in the research. The authors also thank all their collaborators, particularly Geoffrey K. Aguirre, Gustavo D. Aguirre, William A. Beltran, Shannon E. Boye, Sanford L. Boye, Alexander M. Dizhoor, Gerald A. Fishman, William W. Hauswirth, Elise Heon, Edwin M. Stone, and Anand Swaroop for their contributions in helping better understand human CEP290 and GUCY2D retinopathies.

Supported by grants from ProQR Therapeutics, Sanofi Genzyme, National Institutes of Health, Macula Vision Research Foundation, The Chatlos Foundation, Hope for Vision, Foundation Fighting Blindness, and Research to Prevent Blindness.

Disclosure: **A.V. Cideciyan**, ProQR (F), Sanofi Genzyme (F); **S.G. Jacobson,** ProQR (F), Sanofi Genzyme (F)

References

1. Bramall AN, Wright AF, Jacobson SG, McInnes RR. The genomic, biochemical, and cellular responses of the retina in inherited photoreceptor degenerations and prospects for the treatment of these disorders. *Annu Rev Neurosci*. 2010; 33:441–472.
2. Wright AF, Chakarova CF, Abd El-Aziz MM, Bhattacharya SS. Photoreceptor degeneration: genetic and mechanistic dissection of a complex trait. *Nat Rev Genet*. 2010;11:273–284.
3. Daiger SP, Sullivan LS, Bowne SJ. Genes and mutations causing retinitis pigmentosa. *Clin Genet*. 2013;84:132–141.
4. Stone EM, Andorf JL, Whitmore SS, et al. Clinically focused molecular investigation of 1000 consecutive families with inherited retinal disease. *Ophthalmology*. 2017;124:1314–1331.
5. Haider NB, Jacobson SG, Cideciyan AV, et al. Mutation of a nuclear receptor gene, NR2E3, causes enhanced S cone syndrome, a disorder of retinal cell fate. *Nat Genet*. 2000;24: 127–131.
6. Jacobson SG, Cideciyan AV, Aleman TS, et al. Crumbs homolog 1 (CRB1) mutations result in a thick human retina with abnormal lamination. *Hum Mol Genet*. 2003;12:1073–1078.
7. Van Hooser JP, Aleman TS, He YG, et al. Rapid restoration of visual pigment and function with oral retinoid in a mouse model of childhood blindness. *Proc Natl Acad Sci U S A*. 2000;97:8623–8628.
8. Guziewicz KE, Cideciyan AV, Beltran WA, et al. BEST1 gene therapy corrects a diffuse retina-wide microdetachment modulated by light exposure. *Proc Natl Acad Sci U S A*. 2018;115:E2839–E2848.
9. Jacobson SG, Roman AJ, Aleman TS, et al. Normal central retinal function and structure preserved in retinitis pigmentosa. *Invest Ophthalmol Vis Sci*. 2010;51:1079–1085.
10. Sauer CG, Gehrig A, Warneke-Wittstock R, et al. Positional cloning of the gene associated with X-linked juvenile retinoschisis. *Nat Genet*. 1997;17:164–170.
11. Sacchetti M, Mantelli F, Merlo D, Lambiase A. Systematic review of randomized clinical trials on safety and efficacy of pharmacological and nonpharmacological treatments for retinitis pigmentosa. *J Ophthalmol*. 2015;737053:1–11.
12. Gu SM, Thompson DA, Srikumari CR, et al. Mutations in RPE65 cause autosomal recessive childhood-onset severe retinal dystrophy. *Nat Genet*. 1997;17:194–197.
13. Redmond TM, Yu S, Lee E, et al. Rpe65 is necessary for production of 11-cis-vitamin A in the retinal visual cycle. *Nat Genet*. 1998;20:344–351.
14. Acland GM, Aguirre GD, Ray J, et al. Gene therapy restores vision in a canine model of childhood blindness. *Nat Genet*. 2001;28:92–95.
15. Acland GM, Aguirre GD, Bennett J, et al. Long-term restoration of rod and cone vision by single dose rAAV-mediated gene transfer to the retina in a canine model of childhood blindness. *Mol Ther*. 2005;12:1072–1082.
16. Jacobson SG, Aleman TS, Cideciyan AV, et al. Identifying photoreceptors in blind eyes caused by RPE65 mutations: prerequisite for human gene therapy success. *Proc Natl Acad Sci U S A*. 2005;102:6177–6182.
17. Jacobson SG, Acland GM, Aguirre GD, et al. Safety of recombinant adeno-associated virus type 2-RPE65 vector delivered by ocular subretinal injection. *Mol Ther*. 2006;13: 1074–1084.
18. Jacobson SG, Boye SL, Aleman TS, et al. Safety in nonhuman primates of ocular AAV2-RPE65, a candidate treatment for blindness in Leber congenital amaurosis. *Hum Gene Ther*. 2006;17:845–858.
19. Jacobson SG, Aleman TS, Cideciyan AV, et al. Human cone photoreceptor dependence on RPE65 isomerase. *Proc Natl Acad Sci U S A*. 2007;104:15123–15128.
20. Maguire AM, Simonelli F, Pierce EA, et al. Safety and efficacy of gene transfer for Leber's congenital amaurosis. *N Engl J Med*. 2008;358:2240–2248.

21. Bainbridge JW, Smith AJ, Barker SS, et al. Effect of gene therapy on visual function in Leber's congenital amaurosis. *N Engl J Med*. 2008;358:2231–2239.
22. Cideciyan AV, Aleman TS, Boye SL, et al. Human gene therapy for RPE65 isomerase deficiency activates the retinoid cycle of vision but with slow rod kinetics. *Proc Natl Acad Sci U S A*. 2008;105:15112–15117.
23. Hauswirth WW, Aleman TS, Kaushal S, et al. Treatment of Leber congenital amaurosis due to RPE65 mutations by ocular subretinal injection of adeno-associated virus gene vector: short-term results of a phase I trial. *Hum Gene Ther*. 2008;19: 979–990.
24. Cideciyan AV, Hauswirth WW, Aleman TS, et al. Vision 1 year after gene therapy for Leber's congenital amaurosis. *N Engl J Med*. 2009;361:725–727.
25. Cideciyan AV. Leber congenital amaurosis due to RPE65 mutations and its treatment with gene therapy. *Prog Retin Eye Res*. 2010;29:398–427.
26. Jacobson SG, Cideciyan AV, Ratnakaram R, et al. Gene therapy for Leber congenital amaurosis caused by RPE65 mutations: safety and efficacy in 15 children and adults followed up to 3 years. *Arch Ophthalmol*. 2012;130:9–24.
27. Cideciyan AV, Jacobson SG, Beltran WA, et al. Human retinal gene therapy for Leber congenital amaurosis shows advancing retinal degeneration despite enduring visual improvement. *Proc Natl Acad Sci U S A*. 2013;110:E517–E525.
28. Cideciyan AV, Aguirre GK, Jacobson SG, et al. Pseudo-fovea formation after gene therapy for RPE65-LCA. *Invest Ophthalmol Vis Sci*. 2015;56:526–537.
29. Jacobson SG, Cideciyan AV, Roman AJ, et al. Improvement and decline in vision with gene therapy in childhood blindness. *N Engl J Med*. 2015;372:1920–1926.
30. Bainbridge JW, Mehat MS, Sundaram V, et al. Long-term effect of gene therapy on Leber's congenital amaurosis. *N Engl J Med*. 2015;372:1887–1897.
31. Russell S, Bennett J, Wellman JA, et al. Efficacy and safety of voretigene neparvovec (AAV2-hRPE65v2) in patients with RPE65-mediated inherited retinal dystrophy: a randomised, controlled, open-label, phase 3 trial. *Lancet*. 2017;390:849–860.
32. Kotterman MA, Schaffer DV. Engineering adeno-associated viruses for clinical gene therapy. *Nat Rev Genet*. 2014;15: 445–451.
33. Cideciyan AV, Hood DC, Huang Y, et al. Disease sequence from mutant rhodopsin allele to rod and cone photoreceptor degeneration in man. *Proc Natl Acad Sci U S A*. 1998;95: 7103–7108.
34. Cideciyan AV, Charng J, Roman AJ, et al. Progression in X-linked retinitis pigmentosa due to ORF15-RPGR mutations: assessment of localized vision changes over 2 years. *Invest Ophthalmol Vis Sci*. 2018;59:4558–4566.
35. Jacobson SG, Cideciyan AV, Sumaroka A, et al. Outcome measures for clinical trials of Leber congenital amaurosis caused by the intronic mutation in the CEP290 gene. *Invest Ophthalmol Vis Sci*. 2017;58:2609–2622.
36. Jacobson SG, Cideciyan AV, Aguirre GD, et al. Improvement in vision: a new goal for treatment of hereditary retinal degenerations. *Expert Opin Orphan Drugs*. 2015;3:563–575.
37. Ghazi NG, Abboud EB, Nowilaty SR, et al. Treatment of retinitis pigmentosa due to MERTK mutations by ocular subretinal injection of adeno-associated virus gene vector: results of a phase I trial. *Hum Genet*. 2016;135:327–343.
38. Cideciyan AV, Aleman TS, Jacobson SG, et al. Centrosomal-ciliary gene CEP290/NPHP6 mutations result in blindness with unexpected sparing of photoreceptors and visual brain: implications for therapy of Leber congenital amaurosis. *Hum Mutat*. 2007;28:1074–1083.
39. Cideciyan AV, Rachel RA, Aleman TS, et al. Cone photoreceptors are the main targets for gene therapy of NPHP5 (IQCB1) or NPHP6 (CEP290) blindness: generation of an all-cone Nphp6 hypomorph mouse that mimics the human retinal ciliopathy. *Hum Mol Genet*. 2011;20:1411–1423.
40. Jacobson SG, Sumaroka A, Luo X, Cideciyan AV. Retinal optogenetic therapies: clinical criteria for candidacy. *Clin Genet*. 2013;84:175–182.
41. Boye SE, Huang WC, Roman AJ, et al. Natural history of cone disease in the murine model of Leber congenital amaurosis due to CEP290 mutation: determining the timing and expectation of therapy. *PLoS One*. 2014;9:e92928.
42. Jacobson SG, Cideciyan AV, Huang WC, et al. Leber congenital amaurosis: genotypes and retinal structure phenotypes. *Adv Exp Med Biol*. 2016;854:169–175.
43. Downs LM, Scott EM, Cideciyan AV, et al. Overlap of abnormal photoreceptor development and progressive degeneration in Leber congenital amaurosis caused by NPHP5 mutation. *Hum Mol Genet*. 2016;25:4211–4226.
44. Jacobson SG, Cideciyan AV, Sumaroka A. Defining outcomes for clinical trials of Leber congenital amaurosis caused by GUCY2D mutations. *Am J Ophthalmol*. 2017;177:44–57.
45. Charng J, Jacobson SG, Heon E, et al. Pupillary light reflexes in severe photoreceptor blindness isolate the melanopic component of intrinsically photosensitive retinal ganglion cells. *Invest Ophthalmol Vis Sci*. 2017;58:3215–3224.
46. Barrong SD, Chaitin MH, Fliesler SJ, et al. Ultrastructure of connecting cilia in different forms of retinitis pigmentosa. *Arch Ophthalmol*. 1992;110:706–710.
47. Estrada-Cuzcano A, Roepman R, Cremers FP, et al. Non-syndromic retinal ciliopathies: translating gene discovery into therapy. *Hum Mol Genet*. 2012;21:R111–R124.
48. Bujakowska KM, Liu Q, Pierce EA. Photoreceptor cilia and retinal ciliopathies. *Cold Spring Harb Perspect Biol*. 2017;9: a028274.
49. den Hollander AI, Roepman R, Koenekoop RK, Cremers FP. Leber congenital amaurosis: genes, proteins and disease mechanisms. *Prog Retin Eye Res*. 2008;27:391–419.
50. den Hollander AI. Omics in ophthalmology: advances in genomics and precision medicine for Leber congenital amaurosis and age-related macular degeneration. *Invest Ophthalmol Vis Sci*. 2016;57:1378–1387.
51. Kumaran N, Moore AT, Weleber RG, Michaelides M. Leber congenital amaurosis/early-onset severe retinal dystrophy: clinical features, molecular genetics and therapeutic interventions. *Br J Ophthalmol*. 2017;101:1147–1154.
52. Rachel RA, Yamamoto EA, Dewanjee MK, et al. CEP290 alleles in mice disrupt tissue-specific cilia biogenesis and recapitulate features of syndromic ciliopathies. *Hum Mol Genet*. 2015;24: 3775–3791.
53. Khanna H. Photoreceptor sensory cilium: traversing the ciliary gate. *Cells*. 2015;4:674–686.
54. Cremers FP, van den Hurk JA, den Hollander AI. Molecular genetics of Leber congenital amaurosis. *Hum Mol Genet*. 2002;11:1169–1176.
55. den Hollander AI, Koenekoop RK, Yzer S, et al. Mutations in the CEP290 (NPHP6) gene are a frequent cause of Leber congenital amaurosis. *Am J Hum Genet*. 2006;79:556–561.
56. Perrault I, Delphin N, Hanein S, et al. Spectrum of NPHP6/CEP290 mutations in Leber congenital amaurosis and delineation of the associated phenotype. *Hum Mutat*. 2007; 28:416.
57. Walia S, Fishman GA, Jacobson SG, et al. Visual acuity in patients with Leber's congenital amaurosis and early childhood-onset retinitis pigmentosa. *Ophthalmology*. 2010;117: 1190–1198.

Investigative Ophthalmology & Visual Science

58. Yzer S, Hollander AI, Lopez I, et al. Ocular and extra-ocular features of patients with Leber congenital amaurosis and mutations in CEP290. *Mol Vis*. 2012;18:412–425.
59. McAnany JJ, Genead MA, Walia S, et al. Visual acuity changes in patients with Leber congenital amaurosis and mutations in CEP290. *JAMA Ophthalmol*. 2013;131:178–182.
60. Sheck L, Davies WIL, Moradi P, et al. Leber congenital amaurosis associated with mutations in CEP290, clinical phenotype, and natural history in preparation for trials of novel therapies. *Ophthalmology*. 2018;125:894–903.
61. Valkenburg D, van Cauwenbergh C, Lorenz B, et al. Clinical characterization of 66 patients with congenital retinal disease due to the deep-intronic c.2991+1655A>G mutation in CEP290. *Invest Ophthalmol Vis Sci*. 2018;59:4384–4391.
62. Jacobson SG, Aleman TS, Cideciyan AV, et al. Defining the residual vision in Leber congenital amaurosis caused by RPE65 mutations. *Invest Ophthalmol Vis Sci*. 2009;50:2368–2375.
63. Chung DC, Bertelsen M, Lorenz B, et al. The natural history of inherited retinal dystrophy due to biallelic mutations in the RPE65 gene. *Am J Ophthalmol*. 2019;199:58–70.
64. Roman AJ, Schwartz SB, Aleman TS, et al. Quantifying rod photoreceptor-mediated vision in retinal degenerations: dark-adapted thresholds as outcome measures. *Exp Eye Res*. 2005;80:259–272.
65. Roman AJ, Cideciyan AV, Aleman TS, Jacobson SG. Full-field stimulus testing (FST) to quantify visual perception in severely blind candidates for treatment trials. *Physiol Meas*. 2007;28:N51–N56.
66. Collison FT, Park JC, Fishman GA, et al. Full-field pupillary light responses, luminance thresholds, and light discomfort thresholds in CEP290 Leber congenital amaurosis patients. *Invest Ophthalmol Vis Sci*. 2015;56:7130–7136.
67. Huang Y, Cideciyan AV, Papastergiou GI, et al. Relation of optical coherence tomography to microanatomy in normal and rd chickens. *Invest Ophthalmol Vis Sci*. 1998;39:2405–2416.
68. Cideciyan AV, Hufnagel RB, Carroll J, et al. Human cone visual pigment deletions spare sufficient photoreceptors to warrant gene therapy. *Hum Gene Ther*. 2013;24:993–1006.
69. Srinivasan VJ, Monson BK, Wojtkowski M, et al. Characterization of outer retinal morphology with high-speed, ultrahigh-resolution optical coherence tomography. *Invest Ophthalmol Vis Sci*. 2008;49:1571–1579.
70. Spaide RF, Curcio CA. Anatomical correlates to the bands seen in the outer retina by optical coherence tomography: literature review and model. *Retina*. 2011;31:1609–1619.
71. Jonnal RS, Kocaoglu OP, Zawadzki RJ, et al. The cellular origins of the outer retinal bands in optical coherence tomography images. *Invest Ophthalmol Vis Sci*. 2014;55:7904–7918.
72. Staurenghi G, Sadda S, Chakravarthy U, Spaide RF; International Nomenclature for Optical Coherence Tomography (IN•OCT) Panel. Proposed lexicon for anatomic landmarks in normal posterior segment spectral-domain optical coherence tomography: the IN•OCT consensus. *Ophthalmology*. 2014;121:1572–1578.
73. Léveillard T, Sahel JA. Rod-derived cone viability factor for treating blinding diseases: from clinic to redox signaling. *Sci Transl Med*. 2010;2:26ps16.
74. Dacey DM, Liao HW, Peterson BB, et al. Melanopsin-expressing ganglion cells in primate retina signal colour and irradiance and project to the LGN. *Nature*. 2005;433:749–754.
75. McDougal DH, Gamlin PD. The influence of intrinsically-photosensitive retinal ganglion cells on the spectral sensitivity and response dynamics of the human pupillary light reflex. *Vision Res*. 2010;50:72–87.
76. Trapani I, Auricchio A. Seeing the light after 25 years of retinal gene therapy. *Trends Mol Med*. 2018;24:669–681.
77. Ruan GX, Barry E, Yu D, Lukason M, Cheng SH, Scaria A. CRISPR/Cas9-mediated genome editing as a therapeutic approach for Leber congenital amaurosis 10. *Mol Ther*. 2017;25:331–341.
78. Burnight ER, Gupta M, Wiley LA, et al. Using CRISPR-Cas9 to generate gene-corrected autologous iPSCs for the treatment of inherited retinal degeneration. *Mol Ther*. 2017;25:1999–2013.
79. Baye LM, Patrinostro X, Swaminathan S, et al. The N-terminal region of centrosomal protein 290 (CEP290) restores vision in a zebrafish model of human blindness. *Hum Mol Genet*. 2011;20:1467–1477.
80. Zhang W, Li L, Su Q, Gao G, Khanna H. Gene therapy using a miniCEP290 fragment delays photoreceptor degeneration in a mouse model of Leber congenital amaurosis. *Hum Gene Ther*. 2018;29:42–50.
81. Mookherjee S, Chen HY, Isgrig K, et al. A CEP290 C-terminal domain complements the mutant CEP290 of rd16 mice in trans and rescues retinal degeneration. *Cell Rep*. 2018;25:611–623.
82. Burnight ER, Wiley LA, Drack AV, et al. CEP290 gene transfer rescues Leber congenital amaurosis cellular phenotype. *Gene Ther*. 2014;21:662–672.
83. Allocca M, Doria M, Petrillo M, et al. Serotype-dependent packaging of large genes in adeno-associated viral vectors results in effective gene delivery in mice. *J Clin Invest*. 2008;118:1955–1964.
84. Collin RW, den Hollander AI, van der Velde-Visser SD, et al. Antisense oligonucleotide (AON)-based therapy for Leber congenital amaurosis caused by a frequent mutation in CEP290. *Mol Ther Nucleic Acids*. 2012;1:e14.
85. Gerard X, Perrault I, Hanein S, et al. AON-mediated exon skipping restores ciliation in fibroblasts harboring the common Leber congenital amaurosis CEP290 mutation. *Mol Ther Nucleic Acids*. 2012;1:e29.
86. Dulla K, Aguila M, Lane A, et al. Splice-modulating oligonucleotide QR-110 restores CEP290 mRNA and function in human c.2991+1655A>G LCA10 models. *Mol Ther Nucleic Acids*. 2018;12:730–740.
87. Cideciyan AV, Jacobson SG, Drack AV, et al. Effect of an intravitreal antisense oligonucleotide on vision in Leber congenital amaurosis due to a photoreceptor cilium defect. *Nat Med*. 2019;25:225–228.
88. van Soest S, Westerveld A, de Jong PT, Bleeker-Wagemakers EM, Bergen AA. Retinitis pigmentosa: defined from a molecular point of view. *Surv Ophthalmol*. 1999;43:321–334.
89. Veleri S, Lazar CH, Chang B, et al. Biology and therapy of inherited retinal degenerative disease: insights from mouse models. *Dis Model Mech*. 2015;8:109–129.
90. Perrault I, Rozet JM, Calvas P, et al. Retinal-specific guanylate cyclase gene mutations in Leber's congenital amaurosis. *Nat Genet*. 1996;14:461–464.
91. Boye SE. Insights gained from gene therapy in animal models of retGC1 deficiency. *Front Mol Neurosci*. 2014;7:43.
92. Jacobson SG, Cideciyan AV, Peshenko IV, et al. Determining consequences of retinal membrane guanylyl cyclase (RetGC1) deficiency in human Leber congenital amaurosis en route to therapy: residual cone-photoreceptor vision correlates with biochemical properties of the mutants. *Hum Mol Genet*. 2013;22:168–183.
93. Aguirre GK, Butt OH, Datta R, et al. Postretinal structure and function in severe congenital photoreceptor blindness caused by mutations in the GUCY2D gene. *Invest Ophthalmol Vis Sci*. 2017;58:959–973.
94. Boye SE, Boye SL, Pang J, et al. Functional and behavioral restoration of vision by gene therapy in the guanylate cyclase-1 (GC1) knockout mouse. *PLoS One*. 2010;5:e11306.

Investigative Ophthalmology & Visual Science

95. Boye SL, Conlon T, Erger K, et al. Long-term preservation of cone photoreceptors and restoration of cone function by gene therapy in the guanylate cyclase-1 knockout (GC1KO) mouse. *Invest Ophthalmol Vis Sci*. 2011;52:7098–7108.
96. Mihelec M, Pearson RA, Robbie SJ, et al. Long-term preservation of cones and improvement in visual function following gene therapy in a mouse model of leber congenital amaurosis caused by guanylate cyclase-1 deficiency. *Hum Gene Ther*. 2011;22:1179–1190.
97. Boye SL, Peshenko IV, Huang WC, et al. AAV-mediated gene therapy in the guanylate cyclase (RetGC1/RetGC2) double knockout mouse model of Leber congenital amaurosis. *Hum Gene Ther*. 2013;24:189–202.
98. Manfredi A, Marrocco E, Puppo A, et al. Combined rod and cone transduction by adeno-associated virus 2/8. *Hum Gene Ther*. 2013;24:982–992.
99. Boye SL, Peterson JJ, Choudhury S, et al. Gene therapy fully restores vision to the all-cone Nrl(-/-) Gucy2e(-/-) mouse model of Leber congenital amaurosis-1. *Hum Gene Ther*. 2015;26:575–592.

Investigative Ophthalmology & Visual Science